Depth profiling of marker layers using x-ray waveguide structures

Ajay Gupta,[1] Parasmani Rajput,[1] Amit Saraiya,[1] V. R. Reddy,[1] Mukul Gupta,[2] Sigrid Bernstorff,[3] and H. Amenitsch[4]
[1]*UGC-DAE Consortium for Scientific Research, University Campus, Khandwa Road, Indore 452017, India*
[2]*Laboratory for Neutron Scattering, ETHZ and PSI, CH-5232 Villigen PSI, Switzerland*
[3]*Sincrotrone Trieste, SS 14, Km 163.5, I-34012 Basovizza, Trieste, Italy*
[4]*Institute for Biophysics and X-ray Structure Research, Austrian Academy of Sciences, A-8010 Graz, Austria*
(Received 5 April 2005; revised manuscript received 27 May 2005; published 24 August 2005)

It is demonstrated that x-ray waveguide structures can be used for depth profiling of a marker layer inside the guiding layer with an accuracy of better than 0.2 nm. A combination of x-ray fluorescence and x-ray reflectivity measurements can provide detailed information about the structure of the guiding layer. The position and thickness of the marker layer affect different aspects of the angle-dependent x-ray fluorescence pattern, thus making it possible to determine the structure of the marker layer in an unambiguous manner. As an example, effects of swift heavy ion irradiation on a Si/M/Si trilayer (M=Fe, W), forming the cavity of the waveguide structure, have been studied. It is found that in accordance with the prediction of thermal spike model, Fe is much more sensitive to swift heavy ion induced modifications as compared to W, even in thin film form. However, a clear evidence of movement of the Fe marker layer towards the surface is observed after irradiation, which cannot be understood in terms of the thermal spike model alone.

DOI: 10.1103/PhysRevB.72.075436 PACS number(s): 61.10.Eq, 78.70.En, 61.80.Jh

I. INTRODUCTION

X-ray waveguides have attracted a great deal of attention in recent years because of their possible application in x-ray optics for producing intense coherent x-ray beams with a vertical cross section ranging typically from 200 nm to 10 nm, which in turn have applications in microbeam x-ray spectroscopy, diffraction or imaging experiments.[1–7] It has also been demonstrated that x-ray waveguide structures provide a powerful tool to study the structural properties of the guiding layer itself.[5,9–11] The excitation of waveguide modes in planar structures was demonstrated by Feng *et al.*,[1] where a resonance enhancement of the intensity by 20-fold was observed inside the waveguide cavity consisting of a polyimide film sandwiched between Si substrate and SiO_2 top layer. Resonance modes of such a planar waveguide are excited for angle of incidence of x rays satisfying the condition $\theta_i = \theta_m \equiv (m+1)\pi/kW$, where k is the propagation vector of the x-rays and W is the width of the cavity, and m is an integer. Under this condition the mth transverse electric mode of the waveguide is excited, which propagates undisturbed along its length. Various alternative structures have also been suggested in the literature in order to achieve a two-dimensionally confined field,[6] or for producing beams with desired intensity distribution.[7] Waveguides based on Bragg reflection from multilayers instead of total external reflection from high Z element has also been suggested.[8] Zwanenburg *et al.*, demonstrated coherent propagation of x rays in a planar waveguide with a tunable air gap.[5] It was shown that such a structure could be used to do coherent x-ray scattering experiments on a medium filled inside the cavity.[9] Resonance enhancement of the x-ray wave field inside the cavity has been used in order to study weak scattering from macromolecular films.[10]

In the present work we demonstrate that planar x-ray waveguide structures can be used for accurate depth profiling of thin marker layers. The depth resolution can be significantly increased as compared to that achievable using x-ray standing waves generated by total external reflection from a bottom layer of a high Z element.[12,13] Depth profiling of a marker layer is required in a variety of studies including diffusion measurements,[14,15] heavy ion induced material modification,[16,17] etc. As an application of the technique, swift heavy ion induced intermixing in Si/M (M=Fe, W) thin films has been studied. In recent years swift heavy ion irradiation has been used for controlled modification of thin film and multilayer structures. In metallic systems swift heavy ions are known to produce damage above certain threshold electron energy loss S_e, which varies significantly from metal to metal.[18] Since for S_e value close to the threshold, the induced modifications are expected to be small, the present technique can be usefully applied to study the same, which in turn is expected to provide important clues about the mechanism of swift heavy ion induced modifications. The marker layers of Fe and W are chosen because the two metals are known to have very different sensitivity for electronic energy loss.[18] It would be interesting to see if this relative sensitivity of the two metals to swift heavy ions is also maintained in the thin film form.

II. EXPERIMENTAL DETAILS

Waveguide structures were deposited on float glass substrate using electron beam evaporation in an UHV environment with the base pressure in the chamber being 3×10^{-9} mbar. X-ray reflectivity measurements were done using a Siemens D5000 diffractometer with Cu K_α radiation. X-ray fluorescence measurements were done at the SAXS beamline of Elettra synchrotron radiation source using 16 keV x rays. Some of the fluorescence measurements were also done using a rotating anode laboratory source equipped with a Si(111) incident beam monochromator in order to se-

 ©2005 The American Physical Society

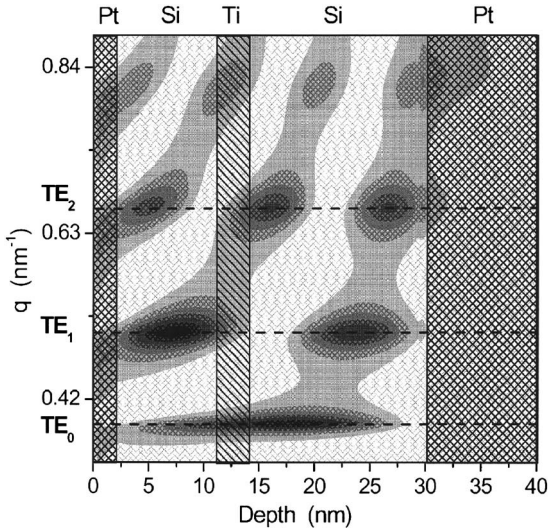

FIG. 1. The contour plot of x-ray field inside the multilayer, substrate/Pt(70 nm)/Si(16 nm)/Ti(3 nm)/Si(9 nm)/Pt(2 nm) as a function of depth and scattering vector q.

lect the $k\alpha_1$ radiation of Cu. Reflected x rays were detected using a gas filled proportional counter, while the fluorescence from the sample was measured using an Amptek XR100T PIN diode detector with an energy resolution of 250 eV. Fluorescence from a Cr foil kept up-stream of the sample was used to correct for the deadtime of the detector.

A multilayer with a nominal structure, float glass (substrate)/Pt(70 nm)/Si(16 nm)/Ti(3 nm)/Si(9 nm)/Pt (2 nm), designated as samples Ti3 was deposited. The two Pt layers form the walls of the planar waveguide while the trilayer Si/Ti/Si forms the guiding layer. The 3 nm thick Ti marker layer is intentionally kept asymmetrically inside the Si cavity, in order to achieve a higher sensitivity in determining its position. In order to demonstrate this point, Fig. 1 gives the contour plot of x-ray intensity inside the multilayer structure as a function of the scattering vector q, calculated using Parratt's formulism.[20] Well localized antinodes of the x-ray standing waves corresponding to TE_0, TE_1 and TE_2 modes of waveguide structure are clearly visible. The position of marker layer is chosen to lie roughly midway between the antinodes corresponding to TE_1 and TE_2 modes. In order to demonstrate how such a structure can improve depth sensitivity, the simulated x-ray fluorescence from the Ti marker layer is shown in Fig. 2 for the following two situations: (i) marker layer lying in the center of the cavity [curve (a)] and (ii) marker layer lying midway between the antinodes corresponding to TE_1 and TE_2 modes [curve (b)]. In the first case, peaks in the fluorescence are observed at q values corresponding to TE_0 and TE_2 modes only. A small shift in the position of the marker layer would result only in a small variation in the intensity of the fluorescence peak corresponding to the TE_2 mode. On the other hand, for the second case, peaks in the fluorescence are observed also corresponding to the TE_1 mode. In the latter case, even a small variation in the depth of the marker layer would result in a significant variation in the relative intensities of fluorescence peaks corresponding to TE_1 and TE_2 modes. This is because at this

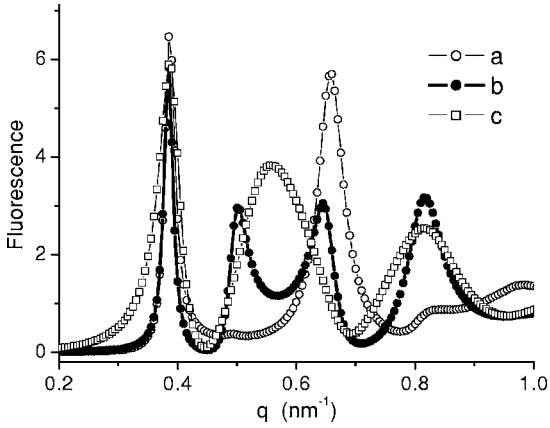

FIG. 2. Simulated x-ray fluorescence from a 3 nm thick Ti marker layer inside the multilayers, (a) substrate/Pt(70 nm)/Si(12.5 nm)/Ti(3 nm)/Si(12.5 nm)/Pt(2 nm); (b) substrate/Pt(70 nm)/Si(15.5 nm)/Ti(3 nm)/Si(9.5 nm)/Pt(2 nm); (c) substrate/Pt(70 nm)/Si(16 nm)/Ti(3 nm)/Si(9 nm).

position the depth distributions of field intensity corresponding to both TE_1 and TE_2 modes have steep gradients with opposite sign. Thus, fitting of the observed relative intensity of the fluorescence peaks corresponding to TE_1 and TE_2 modes would provide a sensitive way to measure the position of the marker layer and any shift in the same due to subsequent sample treatment. For comparison purpose, the simulated fluorescence curve for the second case and without the top Pt layer (i.e., the case of conventional x-ray standing wave structure) is also shown in Fig. 2 [curve (c)]. In this case peaks in fluorescence are observed whenever an antinode scans across the marker layer, and the depth resolution is limited by the width of the antinode.

III. RESULTS AND DISCUSSION

Figure 3(a) gives x-ray reflectivity of the multilayer Ti3 measured using Cu $K\alpha_1$ radiation. Sharp dips in the x-ray reflectivity between θ_c of Si and Pt evidence the excitation of TE_0, TE_1, and TE_2 modes inside the cavity. An attempt to fit the x-ray reflectivity shows that while the simulated pattern is sensitive to the total thickness of the cavity plus the top Pt layer, as well as the interface roughnesses, it is not very sensitive to the position and the width of the Ti marker layer. Figure 3(b) gives the x-ray fluorescence from the Ti marker layer. Fluorescence peaks corresponding to all the three modes are visible. As discussed earlier, the detailed fluorescence pattern depends upon the position of the Ti marker layer. A simultaneous fit of the x-ray reflectivity and the Ti fluorescence pattern was done in order to get the detailed structure of the multilayer. One may note that while the fitting of the first three peaks (corresponding to TE_0, TE_1, and TE_2 modes) is good, the intensity of the fourth peak does not match very well with the theory. This is because of the fact that in the present sample the position of the fourth peak happens to lie close to the critical angle of Pt, and therefore its intensity would be very sensitive to small variations in the electron density or thickness of the Pt layer. Furthermore the

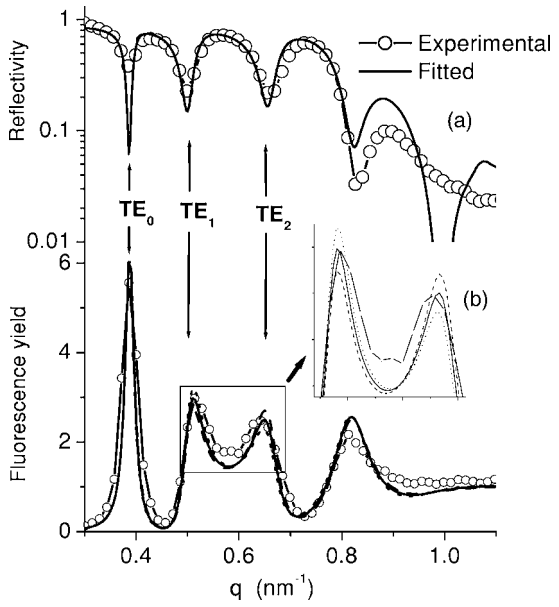

FIG. 3. X-ray reflectivity and Ti fluorescence from the multilayer Ti3 as a function of scattering vector q. The continuous curves represent the best fit to the data. In the inset, simulated curves for Ti position shifted by +0.2 nm (---) and −0.2 nm (…) are also shown.

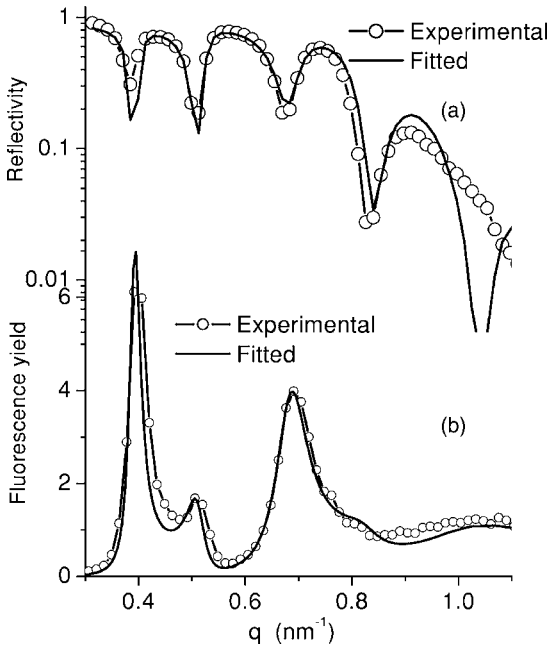

FIG. 4. X-ray reflectivity and Ti fluorescence from the multilayer Ti3s as a function of scattering vector q. The continuous curves represent the best fit to the data.

width of various fluorescence peaks are in general broader than the simulated curves. This is due to the fact that the x-ray beam has a finite divergence, the effect of which has not been incorporated in the simulated spectra. The results of fitting are summarized in Table I. In order to demonstrate the sensitivity of the technique to the position of the marker layer, the inset in Fig. 3(b) shows the simulated patterns corresponding to the position of the marker layer shifted by ±0.2 nm from the best-fit value. These curves clearly mismatch with the experimental data, indicating that the accuracy with which the position of the marker layer can be determined is better than 0.2 nm.

For comparison, x-ray reflectivity and Ti fluorescence from a waveguide structure similar to specimen Ti3, but with Ti layer placed symmetrically inside the guiding layer, i.e., having a structure, float glass (substrate)/Pt(70 nm)/Si(12 nm)/Ti(3 nm)/Si(12 nm)/Pt(2 nm), designated as Ti3s, are given in Figs. 4(a) and 4(b). As expected, x-ray reflectivity evidences the excitation of all TE_0, TE_1, and TE_2 modes; however, in fluorescence measurement, only peaks corresponding to TE_0 and TE_2 are dominant, since for the TE_1 mode, the position of the marker layer almost coincides with a node. A detailed fitting of the data gives the structure of the multilayer as given in Table I. One may note that the marker layer is slightly shifted from the center of the guiding layer, attributable to some variation in the deposition rate. This gives rise to a small peak at the position corresponding to the TE_1 mode.

Next, in the present work it is demonstrated that the thickness of the marker layer sensitively affects the intensity of the peak corresponding to the TE_0 mode. This is due to the fact that the marker layer itself perturbs the field inside the cavity. Thus the observed fluorescence pattern from a sample can be used in an unambiguous determination of the position as well as width of a marker layer.

TABLE I. The results of simultaneous fitting of x-ray reflectivity and x-ray fluorescence data on the multilayer structure. The roughness given is that of the top surface of a layer.

Layer	Sample Ti3		Sample Ti3s		Sample Ti4	
	Thickness (nm)	Roughness (nm)	Thickness (nm)	Roughness (nm)	Thickness (nm)	Roughness (nm)
Pt	1.6±0.1	1.0±0.05	1.6±0.1	1.0±0.05	2.5±0.1	1.5±0.05
Si	9.1	1.0	13.3	1.0	9.2	1.5
Ti	3.0	1.0	3.0	1.0	4.0	1.2
Si	15.9	1.2	10.5	1.2	15.3	1.5
Pt	70.0	1.5	70.0	1.5	70.0	1.5
Substrate		0.5		0.5		0.5

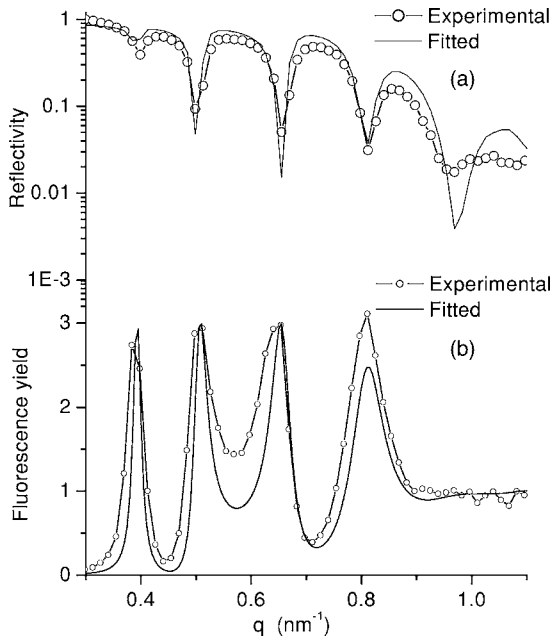

FIG. 5. X-ray reflectivity and Ti fluorescence from the multilayer Ti4 as a function of scattering vector q. The continuous curves represent the best fit to the data.

In order to see the effect of marker layer thickness on the fluorescence pattern, the x-ray reflectivity as well as Ti fluorescence from a multilayer having structure similar to that of Ti3 but with the thickness of the Ti marker layer being equal to 4 nm (designated as Ti4), were also measured, and are shown in Figs. 5(a) and 5(b). In both cases the continuous curves represent the best-fit results obtained by simultaneous fitting of the two data. One may note that, as expected from theoretical simulations, the intensity of the fluorescence peak corresponding to the TE_0 mode is significantly reduced in Ti4. This happens due to the fact that the marker layer itself perturbs the field inside the cavity. The results of fitting are also included in Table I. Thus, while the position of the marker layer mainly affects the intensities of the TE_1 and TE_2 peaks, thickness of the marker layer primarily affects the intensity of the peak corresponding to the TE_0 mode. It may be noted that fitting of experimental data using multiple parameters may not always lead to a unique solution, as a number of different combinations of the parameters may lead to similar quality of fitting. In this context, it is important that in the present case, different parameters of the marker layer affect different aspects of the fluorescence pattern, thus resulting in a more unambiguous determination of the marker structure.

As an application of the technique, swift heavy ion induced intermixing of Si with Fe and W marker layers has been studied. The multilayers having nominal structure, float glass (substrate)/Cr(20 nm)/Au(70 nm)/Si(17 nm)/Fe(4 nm)/Si(12 nm)/Au(2 nm) (designated as Fe4) and float glass(substrate)/Cr(20 nm)/Au(70 nm)/Si(17 nm)/W(1 nm)/Si(12 nm)/Au(2 nm) (designated as W1) were measured before and after irradiation with 100 MeV Au ions to a fluence of 1×10^{13} ions/cm^2. The swift heavy ions are expected to modify the structure of the multilayer. Figures 6 and 7 give the x-ray reflectivity and Fe fluorescence of multilayer Fe4 before and after irradiation. X-ray reflectivity measurements show that the total thickness of the film is reduced after irradiation and the interface roughnesses have increased substantially. On the other hand, x-ray fluorescence measurements show that the relative intensity of the peaks corresponding to the TE_1 and TE_2 modes is significantly altered; before irradiation the intensity of the TE_2 peak was higher than that of the TE_1 peak, while after irradiation the situation is reversed. This suggests that the position of the marker layer got shifted with respect to the center of the guiding layer as a result of irradiation. The results of fitting are given in Table II. Figure 8 compares the electron density profile in the multilayer Fe4 before and after irradiation as obtained from simultaneous fitting of the x-ray reflectivity and Fe fluorescence data. Several features of the irradiation effects may be noted: The concentration profile of the Fe marker layer gets broadened considerably as a result of intermixing with Si, an effect which has been observed in several systems.[16,17,21,22] At the same time, the irradiation result in a contraction of the guiding layer Si/Fe/Si by about 10%, suggesting that the Si layers get densified after irradiation. A decrease in the thickness of the top Au layer after irradiation may be due to electronically mediated sputtering.[19] Perusal of Table II also shows that while in the pristine specimen the position of the Fe marker layer is shifted from the center of the guiding layer by 8.7% of its thickness, after irradiation this shift becomes 9.9%. Thus, the marker layer exhibits an upward movement upon irradiation by $>1\%$ of the layer thickness, which is above the error bars.

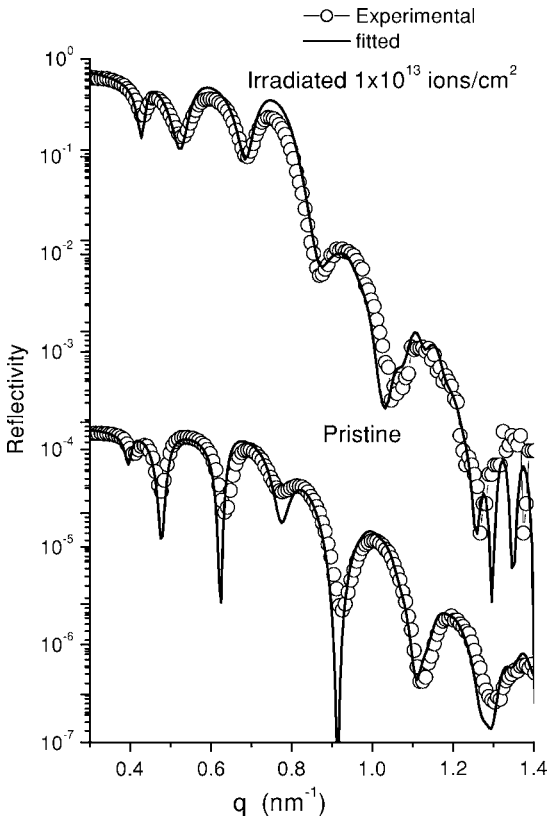

FIG. 6. X-ray reflectivity from multilayer Fe4 before and after irradiation with 100 MeV Au ions (fluence, 1×10^{13} ions/cm^2).

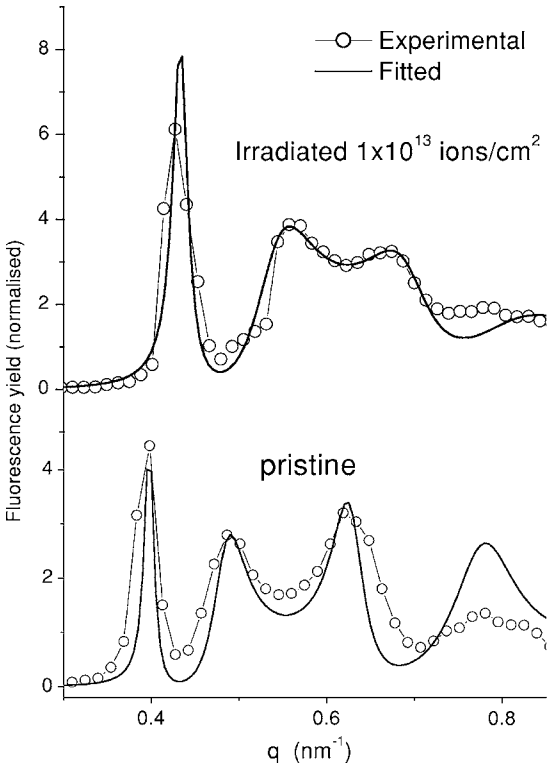

FIG. 7. Fe fluorescence from multilayer Fe4 before and after irradiation with 100 MeV Au ions (fluence, 1×10^{13} ions/cm^2).

In order to compare sensitivity of the W film for swift heavy ion irradiation relative to that of Fe, results of x-ray reflectivity and W fluorescence measurement on multilayer W1 before and after irradiation are shown in Figs. 9 and 10. The results of fitting are included in Table II. Figure 11 gives

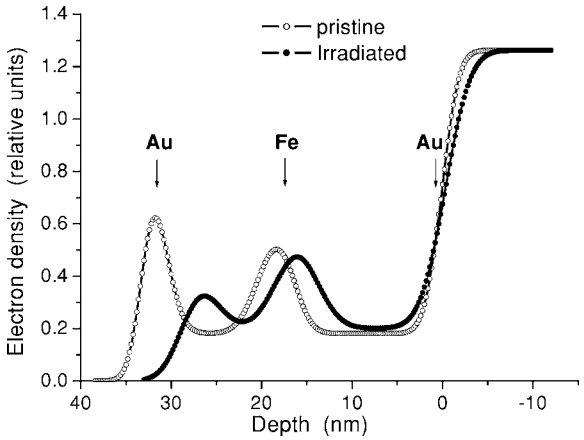

FIG. 8. The electron density profile in multilayer Fe4 before and after irradiation as obtained from simultaneous fitting of x-ray reflectivity and Fe fluorescence data.

the electron density distribution in the multilayer W1 before and after irradiation. One may note that in the case of a W marker layer no appreciable intermixing takes place as a result of irradiation. However, densification of the Si layer is observed in this case also, as evidenced by reduction in the total thickness of the guiding layer. However, in contrast to the Fe layer, position of the W layer relative to the center of the cavity is not shifted.

The above measurements show that while in the Fe-Si system considerable intermixing is observed, in the W-Si system practically no intermixing takes place after irradiation with 100 MeV Au ions. Since Si is common in the two systems, these results show that Fe is much more sensitive to swift heavy ion irradiation as compared to W. This result is in conformity with the thermal spike model,[23,24] and some earlier measurements.[16]

TABLE II. The results of simultaneous fitting of x-ray reflectivity and x-ray fluorescence data on the multilayers Fe4 and W1 before and after irradiation.

Sample	Layer	Before irradiation		After irradiation	
		Thickness (nm)	Roughness (nm)	Thickness (nm)	Roughness (nm)
Fe4	Au	1.7±0.1	1.3±0.05	0.9±0.1	2.0±0.05
	Si	10.9	1.7	8.9	2.3
	Fe	4.0	1.8	4.2	2.2
	Si	16.3	1.5	14.3	2.2
	Au	70.0	1.5	70.0	2.2
	Cr	20.0	1.5	20.0	1.5
	Substrate		0.5		0.5
W1	Au	1.5	2.1	1.3	1.9
	Si	14.2	2.0	13.0	1.8
	W	0.8	1.6	0.8	1.6
	Si	17.5	2.0	16.0	2.3
	Au	70.0	1.5	70.0	1.7
	Cr	20.0	1.5	20.0	1.5
	Substrate		0.5		0.6

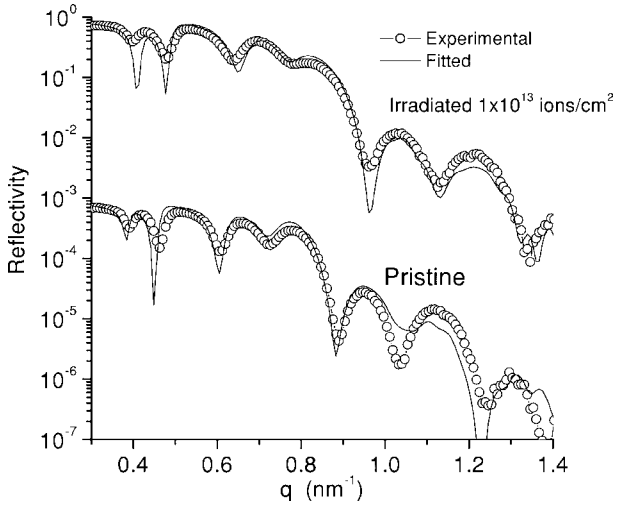

FIG. 9. X-ray reflectivity from multilayer W1 before and after irradiation with 100 MeV Au ions (fluence, 1×10^{13} ions/cm^2).

It may be noted that, in some earlier studies on irradiation of W/Si multilayer with 3.56 GeV ^{238}U ions,[25,26] a strong mixing between W and Si layers, resulting in formation of a W-Si compound, has been observed. However, at this energy of ^{238}U ions, the electronic energy loss in W is 9.7 keV/Å which is well above the threshold damage production in bulk W,[18] and thus is expected to result in intermixing of W and Si layers.

The observed densification of the Si layer in the specimen Fe4 after irradiation may be due either to structural modification of the Si layer or to formation of some Fe-Si phase. However, the fact that even in the Si/W/Si system, the thickness of Si layers is reduced after irradiation, provides a clear evidence that the thickness reduction is due to structural modification of the Si layer. In the present case the Si layers are expected to be amorphous in nature, and therefore would have a large concentration of defects, which can get partially annihilated due to irradiation. Such annihilation of defects due to swift heavy ions has been observed in the literature.[27,18] In some earlier studies crystallization of amorphous Si layer has been observed due to swift heavy ion irradiation above a threshold electronic energy loss, S_e, of about 1.3 keV/Å.[25,28] In the present case S_e in the Si layer is 1.17 keV/Å, which is close to the above threshold value. Therefore crystallization of the amorphous Si layers upon irradiation can also result in densification.

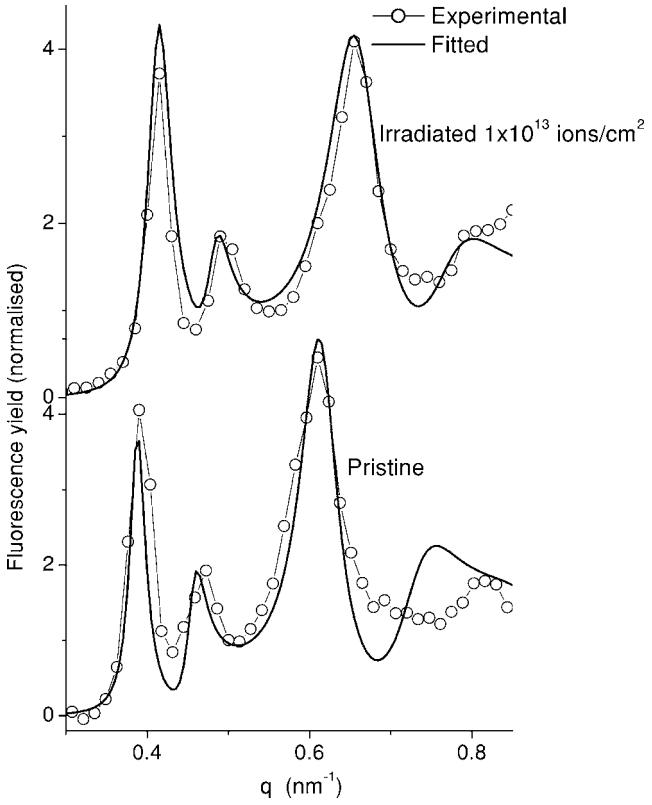

FIG. 10. W fluorescence from multilayer W1 before and after irradiation with 100 MeV Au ions (fluence, 1×10^{13} ions/cm^2).

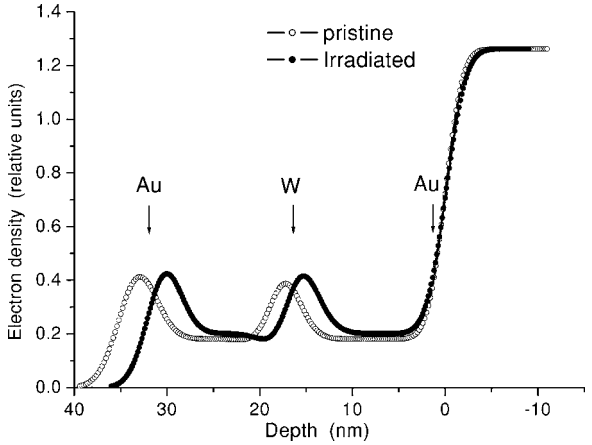

FIG. 11. The electron density profile in multilayer W1 before and after irradiation as obtained from simultaneous fitting of x-ray reflectivity and W fluorescence data.

It is interesting to note that in Si/Fe/Si system Fe layer exhibits a clear shift towards the surface after irradiation. An uneven densification of the Si layers above and below the Fe marker layer may also result in the movement of the Fe layer. However this possibility is unlikely because the energy of the bombarding ion does not change significantly as it traverses through the thickness of the film. Therefore the S_e value in both the Si layer should be the same, and hence the associated effects should also be the same in the two layers. Further, in the Si/W/Si system no such movement of the W marker layer is observed. Thus, this shift is related to S_e induced effects in the marker layer. This effect cannot be understood in terms of the thermal spike model,[23,24] and needs further investigation. Recently, in an interesting experiment, Juraszek *et al.* have studied a possible directional effect of swift heavy ion irradiation in Tb/Fe multilayers by irradiating two identical multilayers kept face to face with each other, thus making the Pb ions traverse the two multilayers in opposite directions (i.e., Tb to Fe and Fe to Tb).[29] Sensitivity to Fe-on-Tb interface was achieved by depositing a 0.5 nm thick ^{57}Fe marker layer at the interface, and using conversion electron Mössbauer spectroscopy to detect the changes at the interface. It was concluded that intermixing at the Fe/Tb interface is not affected by the direction in which

the bombarding ion travels. It may be noted that the effect observed in the present case, i.e., shifting of the position of the marker layer is different from that of a possible asymmetry in the intermixing at the interfaces, and cannot be revealed using techniques like CEMS. Present results demonstrate that the effect of swift heavy ions is not isotropic and has some dependence on the direction of the beam.

IV. CONCLUSIONS

In conclusion, Si/M/Si (M=Ti, Fe, W) trilayer embedded in a planar x-ray waveguide has been studied using x-ray reflectivity and fluorescence measurements. It is shown that the relative intensities of the fluorescence peaks corresponding to the TE_1 and TE_2 modes depend sensitively on the position of the marker layer M, while the intensity of the fluorescence peak corresponding to the TE_0 mode depends on its width. Thus, both position and width of the marker layer can be determined in an unambiguous manner by simultaneous analysis of x-ray reflectivity and fluorescence data. The technique has been used to study the effects of swift heavy ion irradiation in Si/Fe/Si and Si/W/Si systems. The observed effects include (i) intermixing at the interfaces, an effect which has been extensively studied in a number of systems, (ii) densification of the Si layers, which may be attributed to annihilation of defects and/or crystallization of the layers, and (iii) a small shift in the relative position of the marker layer in the case of the Si/Fe/Si system. It is found that in conformity with the thermal spike model, Fe is more sensitive to electronic energy loss induced damage as compared to W. However, the observed shift in the position of the Fe marker layer upon irradiation cannot be understood in terms of the thermal spike model.

ACKNOWLEDGMENT

Thanks are due to Satish Potddar for help in depositing the multilayer structures.

[1] Y. P. Feng, S. K. Sinha, H. W. Deckman, J. B. Hastings, and D. P. Siddons, Phys. Rev. Lett. **71**, 537 (1993).

[2] Y. P. Feng, S. K. Sinha, E. E. Fullerton, G. Grübel, D. Abernathy, D. P. Siddons, and J. B. Hastings, Appl. Phys. Lett. **67**, 3647 (1995); S. Lagomarsino, A. Cedola, P. Cloetens, S. Di Fonzo, W. Jark, G. Soullie, and C. Riekel, *ibid.* **71**, 2557 (1997).

[3] S. Di Fonzo, W. Jark, S. Lagomarsino, C. Giannini, L. De Caro, A. Cedole, and M. Müller, Nature (London) **403**, 638 (2000).

[4] V. K. Egorov and E. V. Egorov, Thin Solid Films **398**, 405 (2001); F. Pfeiffer, T. Salditt, and C. David, J. Appl. Crystallogr. **35**, 430 (2002); J. H. H. Bongaerts, C. David, M. Drakopoulos, M. J. Zwanenburg, G. H. Wegdam, T. Lackner, H. Keymeulen, and J. F. van der Veen, J. Synchrotron Radiat. **9**, 383 (2002).

[5] M. J. Zwanenburg, J. F. Peters, J. H. H. Bongaerts, S. A. de Vries, D. L. Abernathy, and J. F. van der Veen, Phys. Rev. Lett. **82**, 1696 (1999).

[6] F. Pfeiffer, C. David, M. Burghammer, C. Riekel, and T. Salditt, Science **297**, 230 (2002).

[7] F. Pfeiffer, T. Salditt, P. Hoghoj, I. Anderson, and N. Schell, Phys. Rev. B **62**, 16939 (2000).

[8] I. R. Prudnikov, Phys. Rev. B **67**, 233303 (2003).

[9] M. J. Zwanenburg, J. H. H. Bongaerts, J. F. Peters, D. O. Riese, and J. F. van der Veen, Phys. Rev. Lett. **85**, 5154 (2000).

[10] T. Salditt, F. Pfeiffer, H. Perzl, A. Vix, U. Mennicke, A. Jarre, A. Mazuelas, and T. H. Metzger, Physica B **336**,181 (2003); F. Pfeiffer, U. Mennicke, and T. Salditt, J. Appl. Crystallogr. **35**, 163 (2002).

[11] S. Zheludeva, M. Kovalchuk, and N. Novikova, Spectrochim. Acta, Part B **56**, 2019 (2001).

[12] M. J. Bedzyk and L. Cheng, in *Reviews in Mineralogy and Geochemistry*, edited by P. A. Fenter, M. L. Rivers, N. C. Sturchio, and S. R. Sutton (Mineralogical Society of America, Washington, DC) 49, 221 (2002).

[13] S. K. Ghose, B. N. Dev, and Ajay Gupta, Phys. Rev. B **64**, 233403 (2001).

[14] P. F. Green, C. J. Palmstrom, J. W. Mayer, and E. J. Kramer, Macromolecules **18**, 501 (1985).

[15] G. Reiter, S. Huttenbach, M. Foster, and M. Stamm, Macromolecules **24**, 1179 (1991).

[16] Ajay Gupta, Carlo Meneghini, Amit Saraiya, Giovanni Principi, and D. K. Avasthi, Nucl. Instrum. Methods Phys. Res. B **212**, 458 (2003).

[17] G. Schiwietz, E. Luderer, G. Xiao, and P. L. Grande, Nucl. Instrum. Methods Phys. Res. B **175**,1 (2001); Ajay Gupta, Vacuum **58**, 16 (2000).

[18] A. Dunlop, D. Lesueur, P. Legrand, H. Dammak, and J. Dural, Nucl. Instrum. Methods Phys. Res. B **90**, 330 (1994); A. Dunlop and D. Lesueur, Radiat. Eff. Defects Solids **126**, 123 (1993).

[19] Ajay Gupta and D. K. Avasthi, Phys. Rev. B **64**, 155407 (2001).

[20] L. G. Parratt, Phys. Rev. **95**, 359 (1954); S. K. Ghose and B. N. Dev, Phys. Rev. B **63**, 245409 (2001).

[21] K. Diva, D. Kabiraj, B. R. Chakraborty, S. M. Shivaprasad, and D. K. Avasthi, Nucl. Instrum. Methods Phys. Res. B **222**, 169 (2004); C. Jaouen, A. Michel, J. Pacaud, C. Dufour, Ph. Bauer, and B. Gervais, *ibid.* **148**, 176 (1999).

[22] C. Dufour, Ph. Bauer, G. Marchal, J. Grilhe, C. Jaouen, J. Pacaud, and J. C. Jousset, Europhys. Lett. **21**, 671 (1993).

[23] Z. G. Wang, Ch. Dufour, E. Paumier, and M. Toulemonde, J. Phys.: Condens. Matter **6**, 6733 (1994); Z. G. Wang, Ch. Dufour, S. Euphrasie, and M. Toulemonde, Nucl. Instrum. Methods Phys. Res. B **209**, 194 (2003).

[24] M. Toulemonde, J. M. Costantini, Ch. Dufour, A. Meftah, E. Paumier, and F. Studer, Nucl. Instrum. Methods Phys. Res. B **116**, 37 (1996); T. Wiss, H. Matzke, C. Trautmann, M. Toulemonde, and S. Klaumunzer, *ibid.* **122**, 583 (1997).

[25] J. Marfaing, W. Marine, B. Vidal, M. Toulemonde, M. Hage Ali, and J. P. Stoquert, Appl. Phys. Lett. **57**, 1739 (1990).

[26] J. Marfaing, W. Marine, B. Vidal, M. Toulemonde, M. Hage Ali, and J. P. Stoquert, Appl. Surf. Sci. **46**, 422 (1990).

[27] A. Iwase, S. Sasaki, T. Iwata, and T. Nihira, Phys. Rev. Lett. **58**, 2450 (1987).

[28] K. Izui and S. Furuno, in *Proceedings of the XIth International Congress on Electron Microscopy*, Kyoto, 1986, edited by T. Imura, S. Maruse, and T. Suzuki (The Japanese Society of Electron Microscopy, Tokyo, 1986), p. 1299.

[29] J. Juraszek, A. Fnidiki, J. Teillet, M. Toulemonde, A. Michel, and W. Keune, Phys. Rev. B **61**, 12 (2000).